

# Joint image compression and encryption based on order-8 alternating transforms

Peiya Li, Kwok-Tung Lo

*Department of Electronic and Information Engineering, The Hong Kong Polytechnic University, Hung Hom, Kowloon, Hong Kong, China*

---

## Abstract

In this paper, we propose a novel joint image compression and encryption scheme based on JPEG standard. We realize image encryption at JPEG's transformation stage. Instead of only using  $8 \times 8$  discrete cosine transform (DCT) for transformation, we generate new orthogonal transforms by embedding an extra rotation angle of  $\pi$  to different stages' butterflies in  $8 \times 8$  DCT's flow-graph, and then apply them alternatively for transformation according to a predefined secret key. By carefully controlling the number of rotation angles embedded, the quality control of encrypted images can also be achieved. The encryption algorithm is further enhanced by performing block permutation before the entropy encoding stage. Extensive experiments have been conducted to show the good protection and compression performance of our encryption schemes. Finally, a detailed security analysis is provided to show the encryption schemes' resistance to various cryptanalysis methods, such as brute-force attack, key sensitivity analysis, replacement attack and statistical attack.

---

*Email addresses:* yolanda.peiya@connect.polyu.hk (Peiya Li), kwok.tung.lo@polyu.edu.hk (Kwok-Tung Lo)

*Preprint submitted to Vis. Commun. Image R.*

*October 26, 2016*

*Keywords:* Image encryption, orthogonal transforms, security analysis, JPEG standard

---

## 1. Introduction

In recent years, with the rapid development of multimedia technologies, many powerful and interesting new applications have been developed for people to share their images stored in mobile smart devices through different social network platforms, such as Facebook and Instagram. In typical use of images, owners tend to store them for future use or distribute them to the specific people through Internet which is particularly vulnerable to eavesdropping and intercepting, thus there exists a great demand on efficient, secure image storage and transmission. Encryption is one of the common ways to ensure image security.

Until now, there are various cryptographic techniques, like Data Encryption Standard (DES) and Advanced Encryption Standard (AES) [1], but they are designed primarily for text data security. For image encryption using these conventional algorithms, the computational cost will be high because of the large size of image data. Moreover, unlike text data, the information density of images is much lower, and the real-time processing is often required for many image applications, thus an encryption strategy with low computational cost and fast encryption/decryption speed is desired for image safety.

In the past time, scrambling techniques were widely used by researchers to achieve image encryption. These techniques include simple permutation operations and affine transformation operations in the time or frequency do-

23 main [2–5]. However, along with the rapid increasing of computing power,  
24 breaking this kind of encryption schemes becomes much easier. Then, con-  
25 sidering the fact that compression is a must-do step for most images we see  
26 on the Internet, the focus of image security research shifted to integrating  
27 image compression process with encryption, for the purpose of reducing en-  
28 cryption and decryption time in image communication and processing. The  
29 most popular method for this encryption direction is partial encryption or se-  
30 lective encryption, which applies encryption to a portion of coefficients from  
31 either the final results or the intermediate stages of the image compression  
32 system. The major aim of partial image encryption is to reduce the amount  
33 of data for encryption while obtaining a certain level of security.

34 Based on the different processing order of encryption and compression  
35 process, partial image encryption can be divided into three categories: pre-  
36 compression, in-compression, and post-compression [6]. Pre-compression  
37 means performing encryption before compression, and decompression before  
38 decryption. In [7], Tang proposed a method to realize partial image encryp-  
39 tion by encrypting the DC coefficients with DES and randomly permuting  
40 the AC coefficients rather than the standard zigzag scanning order. This  
41 encryption scheme is format compliant to JPEG, but it introduces about  
42 40% loss in compression efficiency, because the new permutation disrupts  
43 the probability distribution of run-lengths, and renders the performance of  
44 Huffman tables less than optimal [8]. For in-compression category, image  
45 encryption/decryption and image compression/decompression are performed  
46 jointly. In [9–11], Wu *et al.* realized partial encryption in the entropy coding  
47 stage by using multiple Huffman tables alternately in a secret order. This

48 encryption scheme can achieve very high-visual degradation without sacri-  
49 ficing the compression performance, but it is not format compliant, because  
50 the decoder needs to decrypt the Huffman table used for encryption in order  
51 to do decompression. Post-compression algorithms perform encryption after  
52 compression, and are generally compression friendly; no modifications are  
53 needed for encryption and decryption at the encoder or decoder side. In [12],  
54 they proposed a JPEG image encryption method by only encrypting those  
55 bits that are used to fully specify the signs and magnitudes of nonzero coef-  
56 ficients in the Huffman coding stage. This algorithm can obtain high-visual  
57 degradation and is format compliant to JPEG, but it is not tunable since its  
58 encryption parameters are static.

59 In [13–16], Au-Yeung *et al.* proposed to realize partial video encryption  
60 by embedding the encryption scheme at the transformation stage during the  
61 encoding process. Since transformation is a must-do step in the video encoder  
62 and decoder, an obvious advantage of this scheme is that it introduces nearly  
63 zero extra computations. They generated a number of new orthogonal trans-  
64 forms with similar coding efficiency to DCT-II by modifying angle values in  
65 DCT-II’s flow-graph structure, and then applied these new transforms alter-  
66 nately according to a predefined secret key to realize partial video encryption.  
67 In [16], they first suggested a simple design to generate new orthogonal trans-  
68 forms by selecting four different sets of rotation angles ( $\theta_1 = \pi/4, \theta_2 = 3\pi/8$ ),  
69 ( $\theta_1 = 3\pi/8, \theta_2 = \pi/4$ ), ( $\theta_1 = 7\pi/24, \theta_2 = 8\pi/24$ ), ( $\theta_1 = 8\pi/24, \theta_2 = 7\pi/24$ ),  
70 at the  $2^{nd}$  stage of the 4-point DCT’s flow-graph structure (shown in Fig. 1).  
71 Then in order to enlarge the differences among these alternative transforms  
72 which can offer a good protection against possible attacker, they achieved the

73 maximum difference in [15] by allowing an extra rotation of  $\pi$  to  $\theta_1$  or/and  
 74  $\theta_2$ . These newly generated transforms have exactly the same coding effi-  
 75 ciency as DCT since they are the sign-flipped version of the original DCT.  
 76 Next, they extended the  $4 \times 4$  transforms based encryption frame-work into  
 77  $8 \times 8$  case [14], which allows more room to do butterflies' sign-flipping and  
 78 thus to embed the encryption. In [14], three different encryption algorithms  
 79 were proposed, and they claimed that *Algorithm-3* could get the best balance  
 80 between the encryption power and coding efficiency.

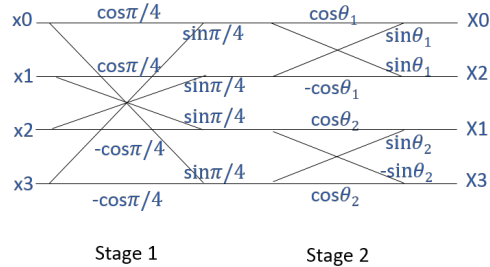


Figure 1: Flow graph of 4-point (1-D) DCT ( $\theta_1 = \pi/4$ ,  $\theta_2 = 3\pi/8$ )

81 In our work, we propose a new joint image compression and encryption  
 82 scheme with controllable image quality by embedding encryption algorithm  
 83 at JPEG's transformation stage. The proposed scheme can achieve a suf-  
 84 ficiently high level of security while maintain the good compression perfor-  
 85 mance of JPEG, and it is format compliant to JPEG standard. Instead of  
 86 using the  $8 \times 8$  DCT alone for transformation, we develop new order-8 or-  
 87 thogonal transforms by adopting the sign-flipping strategy used in [14], but  
 88 the butterflies we do sign-flips are different from [14], resulting in different  
 89 new transform sets for transformation. Then, encryption algorithm using  
 90 the newly generated transform sets is presented. Encryption and compres-

91 sion performances are evaluated through some common judgement criteria.  
92 And we have shown that our new orthogonal transforms have better coding  
93 efficiency than those generated in [14]. By carefully selecting the butter-  
94 flies for angle rotation, we can control the visual quality of the encrypted  
95 images. Additionally, to better resist the direct replacement attack, we mod-  
96 ify the encryption algorithm by adding the block permutation operation. A  
97 detailed security analysis of our proposed encryption scheme is provided fi-  
98 nally to show its resistance to various attacks, such as brute-force attack, key  
99 sensitivity analysis, replacement attack, and statistical analysis.

100 In the rest of the paper, Section 2 introduces the method to generate new  
101 order-8 orthogonal transforms which will be used alternatively for transfor-  
102 mation according to the encryption key in our encryption algorithm. Section  
103 3 describes the encryption/decryption algorithm, evaluate and compare its  
104 performance with JPEG and Au-Yeung's *Algorithm-3* [14], together with  
105 the quality control realization of encrypted images. Section 4 shows the de-  
106 tailed security analysis results of our encryption algorithms. Section 5 gives  
107 a conclusion and presents our future research directions.

## 108 **2. Generation of new order-8 orthogonal transforms**

109 In JPEG,  $8 \times 8$  DCT is used for transformation, because it has proved to  
110 be the best transform in terms of compression ability when the correlation  
111 among inter-pixels is strong — which is actually true in most natural pictures.  
112 In [17], a fast DCT-II algorithm was proposed in the form of matrices and  
113 was illustrated by a signal-flow graph. In our method for generating new  
114 orthogonal transforms, we modify the signal-flow graph structure through

115 introducing extra rotation angle of  $\pi$  to different butterflies. Therefore, we  
 116 first introduce the underlying fast computational algorithm for DCT-II, then  
 117 explain how to generate new transforms based on it.

118 *2.1. One fast computational algorithm for DCT-II*

119 The fast DCT computational algorithm [17] is based upon matrix decom-  
 120 position. In general, an order- $N$  type II DCT matrix can be written into the  
 121 following recursive form:

122

$$\begin{aligned}
 [C_N^{II}] &= [P_N] \begin{bmatrix} P_{N/2}^T C_{N/2}^{II} & 0 \\ 0 & R_{N/2} \end{bmatrix} [B_N], \\
 [B_N] &= \frac{\sqrt{2}}{2} \begin{bmatrix} I_{N/2} & \bar{I}_{N/2} \\ \bar{I}_{N/2} & -I_{N/2} \end{bmatrix},
 \end{aligned} \tag{1}$$

123 where  $[P_N]$  is an  $N \times N$  permutation matrix which permutes the transformed  
 124 vector from a bit reversed order to a natural order.  $[I_{N/2}]$  is the identity  
 125 matrix and  $[\bar{I}_{N/2}]$  is the anti-diagonal identity matrix.  $[R_{N/2}]$  can be de-  
 126 composed into  $(2 \log_2 N - 3)$  matrices.

127 Since in JPEG standard, only order-8 DCT-II is used for transformation,  
 128 here we present the flow-graph of it in Fig. 2, and its fast computational  
 129 formula can be described as:

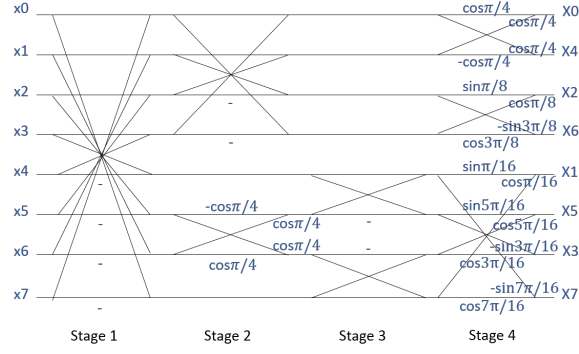


Figure 2: Flow graph of 8-point (1-D) DCT

130

$$\begin{aligned}
 [C_8^{II}] &= [P_8] \begin{bmatrix} P_4^T C_4^{II} & 0 \\ 0 & R_4 \end{bmatrix} [B_8], & (2) \\
 [C_4^{II}] &= [P_4] \begin{bmatrix} P_2^T C_2^{II} & 0 \\ 0 & R_2 \end{bmatrix} [B_4], \\
 [P_4] &= \begin{bmatrix} 1 & 0 & 0 & 0 \\ 0 & 0 & 1 & 0 \\ 0 & 1 & 0 & 0 \\ 0 & 0 & 0 & 1 \end{bmatrix}, \\
 [R_2] &= [M1] = \begin{bmatrix} \sin \frac{\pi}{8} & \cos \frac{\pi}{8} \\ -\sin \frac{\pi}{8} & \cos \frac{\pi}{8} \end{bmatrix}, \\
 [P_2] &= \begin{bmatrix} 1 & 0 \\ 0 & 1 \end{bmatrix}, [C_2^{II}] = \frac{\sqrt{2}}{2} \begin{bmatrix} 1 & 1 \\ 1 & -1 \end{bmatrix},
 \end{aligned}$$



$$[P_8] = \begin{bmatrix} 1 & 0 & 0 & 0 & 0 & 0 & 0 & 0 \\ 0 & 0 & 0 & 0 & 1 & 0 & 0 & 0 \\ 0 & 0 & 1 & 0 & 0 & 0 & 0 & 0 \\ 0 & 0 & 0 & 0 & 0 & 0 & 1 & 0 \\ 0 & 1 & 0 & 0 & 0 & 0 & 0 & 0 \\ 0 & 0 & 0 & 0 & 0 & 1 & 0 & 0 \\ 0 & 0 & 0 & 1 & 0 & 0 & 0 & 0 \\ 0 & 0 & 0 & 0 & 0 & 0 & 0 & 1 \end{bmatrix},$$

$$[R_4] = [M1][M2][M3],$$

where

$$[M1] = \begin{bmatrix} \sin \frac{\pi}{16} & 0 & 0 & \cos \frac{\pi}{16} \\ 0 & \sin \frac{5\pi}{16} & \cos \frac{5\pi}{16} & 0 \\ 0 & -\sin \frac{3\pi}{16} & \cos \frac{3\pi}{16} & 0 \\ -\sin \frac{7\pi}{16} & 0 & 0 & \cos \frac{7\pi}{16} \end{bmatrix},$$

Computation of  $[M1]$  is equivalent to the butterfly denoted in the bottom half of Stage-4 in Fig. 2.

$$[M2] = \frac{\sqrt{2}}{2} \begin{bmatrix} 1 & 1 & 0 & 0 \\ 1 & -1 & 0 & 0 \\ 0 & 0 & -1 & 1 \\ 0 & 0 & 1 & 1 \end{bmatrix},$$

Computation of  $[M2]$  is equivalent to the butterfly denoted in the bottom

half of Stage-3 in Fig. 2.

$$[M3] = \begin{bmatrix} 1 & 0 & 0 & 0 \\ 0 & -\cos \frac{\pi}{4} & \cos \frac{\pi}{4} & 0 \\ 0 & \cos \frac{\pi}{4} & \cos \frac{\pi}{4} & 0 \\ 0 & 0 & 0 & 1 \end{bmatrix},$$

132 Computation of  $[M3]$  is equivalent to the butterfly denoted in the bottom  
 133 half of Stage-2 in Fig. 2.

### 134 2.2. Generation of new orthogonal transforms

135 Considering the encryption and compression performance, the coding ef-  
 136 ficiency of the new generated transforms should either be exactly the same  
 137 to what can be achieved by DCT or just fall slightly. Thus, we do not intro-  
 138 duce angle rotation to butterflies in Stage-1 and Stage-2, because this will  
 139 cause big changes in the transform coefficients, which will eventually affect  
 140 the overall coding efficiency.

141 In our transform generation method, using the extra rotation angle of  $\pi$ ,  
 142 we generate two different sets of new orthogonal transforms,  $TS1$  and  $TS2$ .  
 143  $TS1$  has 16 different orthogonal transforms, generated by introducing sign-  
 144 flips (an extra rotation angle of  $\pi$ ) into the four butterflies at Stage-4 in Fig.  
 145 2, which can be described in the following mathematical formula:

$$146 \quad [C_8^{II}] = [P_8][T_1] \begin{bmatrix} P_4^T C_4^{II} & 0 \\ 0 & R_4 \end{bmatrix} [B_8], \quad (3)$$

147 where  $[T_1] = \text{diag}(\cos \theta_1, \cos \theta_1, \cos \theta_2, \cos \theta_2, \cos \theta_3, \cos \theta_4, \cos \theta_4, \cos \theta_3)$ ,  $\theta_i =$   
 148 0 or  $\pi$  ( $i = 1, 2, 3, \text{ or } 4$ ). Here, the normalized coefficients are ignored. The

149 coding efficiencies of transforms in *TS1* are exactly the same to that of DCT  
 150 because they are just the sign-changed format of the original DCT elements.

151 *TS2* has 64 different orthogonal transforms, generated by introducing  
 152 sign-flips into the four butterflies at Stage-4 and the two butterflies at Stage-  
 153 3 in Fig. 2, which can be described in the following mathematical formula:

154

$$\begin{aligned}
 [C_8^{II}] &= [P_8][T_1] \begin{bmatrix} P_4^T C_4^{II} & 0 \\ 0 & R_4' \end{bmatrix} [B_8], \\
 [R_4'] &= [M1][T_2][M2][M3],
 \end{aligned} \tag{4}$$

155 where  $[T_2] = \text{diag}(\cos \theta_5, \cos \theta_5, \cos \theta_6, \cos \theta_6)$ ,  $\theta_i = 0$  or  $\pi$  ( $i = 5$  or  $6$ ), and the  
 156 normalized coefficients are ignored. The coding efficiency of these transforms  
 157 will be a little lower than that of DCT because some of them will change not  
 158 only coefficients sign, but also their magnitudes after transformation.

### 159 **3. Joint image compression and encryption based on alternating** 160 **transforms**

#### 161 *3.1. Encryption algorithm and experiment results*

162 The encryption scheme can be divided into two parts: 1) random (secret)  
 163 key generation, and 2) alternating transforms according to the secret key.  
 164 For the key generation, we use the RC4 algorithm, which turns to be one of  
 165 the most commonly-used random key generators [18]. The encryption algo-  
 166 rithm is stated as follows:

#### 167 *Encryption Algorithm-1*

168

169 *Step 1:* Initialize the RC4 key generator with a predefined 128-bit key;

170 *Step 2:* For an input  $8 \times 8$  image block, do

171     *Step 2.1:* Get 52 bits from the random generator;

172     *Step 2.2:* Use the first 4 bits to select one transform from *TS1* for

173         *all* rows in the  $1^{st}$  dimension;

174     *Step 2.3:* Use the following  $6 \times 8$  bits to select one transform from

175         *TS2* for *each* column in the  $2^{nd}$  dimension;

176 *Step 3:* Transform each  $8 \times 8$  image block using the selected transforms, then

177     perform JPEG’s quantization and entropy coding procedure;

178 *Step 4:* Repeat *Step 2* and *Step 3* until all  $8 \times 8$  blocks are processed.

---

179

180 In *Algorithm-1*, we use *TS1* and *TS2* together and implement the  $1^{st}$  and

181  $2^{nd}$  dimension transformation separately. These operations will change the

182 transformed coefficients in both signs and magnitudes, thus cryptanalyzing

183 our encrypted images through some sign-flips on the DCT transformed coef-

184 ficients of the same data block is not feasible.

185 For the decryption algorithm, we just follow JPEG’s decoding process

186 by using the encryption key to select the corresponding transforms for de-

187 transformation. In Fig. 3, we present the encrypted image and decrypted

188 image of ‘Lena’, when the quality factor is 20. All images used in our exper-

189 iment are taken from the USC-SIPI image database available on the website

190 “<http://sipi.usc.edu/database>”. We assume that the standard IDCT is al-

191 ways used for decryption when the encryption key is unknown. Performance

192 comparison between our encryption algorithm and the *Algorithm-3* in ref-

193 erence [14] is shown in Fig.4. In Fig. 4(a), we can observe a large PSNR

194 value drop when the encryption key is unknown and only IDCT is used for  
195 decryption, which means a good protection ability of our encryption algo-  
196 rithm. When the encryption key is known, the PSNR value, which reflects  
197 the coding efficiency of transforms, of *Algorithm-1* is more close to that of  
198 JPEG standard than that of the reference paper's algorithm, illustrating that  
199 our transform sets' coding efficiency is better than the transform sets in [14].  
200 For the PSNR-BS (Bit-stream Size) relationship and PSNR-CR (Compres-  
201 sion Ratio) relationship shown in Fig. 4(b) and Fig. 4(c), compared with  
202 JPEG standard, our algorithm also has better compression performance and  
203 smaller bit-stream size than *Algorithm-3* in [14].

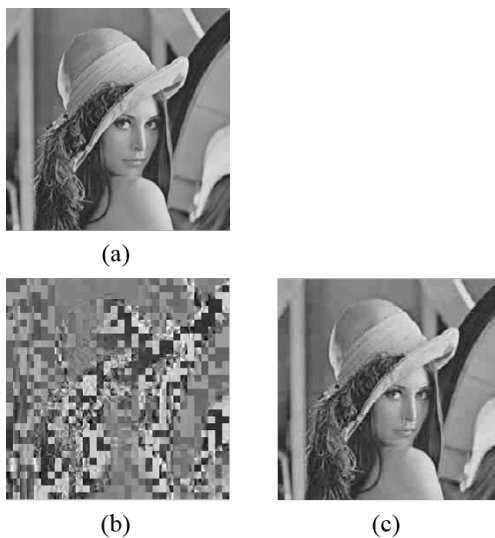


Figure 3: Performance of *Algorithm-1*: (a) plain Lena image, (b) encrypt image, (c) decrypt image

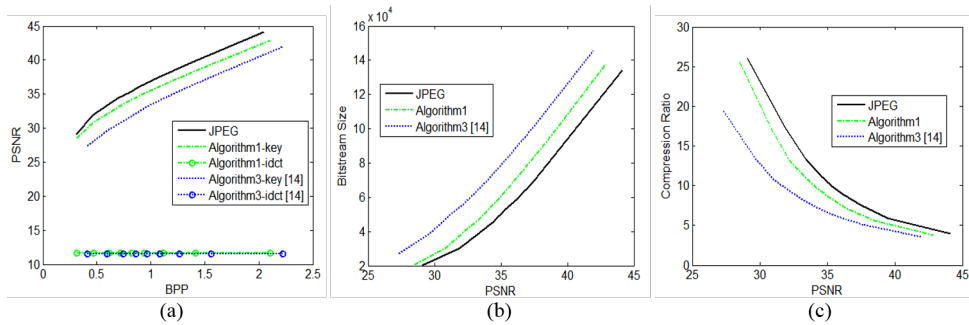


Figure 4: Performance comparison among different encryption algorithms: (a) BPP-PSNR relationship, (b) PSNR-BS relationship, (c) PSNR-CR relationship

### 204 3.2. Quality control of our encryption scheme

205 For partial image encryption, an encrypted image with poor visual quality  
 206 can be generated without the encryption key. However, different applications  
 207 may have different visual quality requirements of the encrypted images, thus  
 208 it is necessary to allow the service provider a chance to control how bad the  
 209 encrypted image quality will be.

210 In our encryption scheme, in order to achieve quality control, instead of  
 211 changing all the four angles in matrix  $[T_1]$ , we select some of them to be  $\pi$   
 212 while keeping the others unchanged. Table 1 has listed the different PSNR  
 213 performances of various selections of  $\theta_i$  ( $i = 1, 2, 3, \text{ or } 4$ ) for encryption. Three  
 214 images are used for testing with quality factor to be 20. From Table 1, it is  
 215 clearly shown that among four rotation angles,  $\theta_1$  has the biggest influence  
 216 on the PSNR value, as it controls the DC component of each  $8 \times 8$  block. In  
 217 Fig. 5, we present the visual results of the three representative selections in  
 218 Table 1 of these three images. It is clearly that the visual qualities of these  
 219 images are quite different, which are consistent with their PSNR values. For

220 example, images in Case (b) are visually much more pleasant than images in  
 221 Case (c) and Case (d). Thus, we can choose whether to change  $\theta_1$  or not to  
 222 obtain high or low encryption ability, and change other three rotation angles  
 223 to make some fine adjustment on the quality of images.

Table 1: PSNR [dB] performance of various selection of  $\theta_i$  for encryption

Image Angle change	Lena	Aerial	Peppers
None (a)	31.9051	28.3087	32.4234
Stage-3 (b)	22.8940	19.0769	23.7966
Stage-3 & $\theta_1$	11.5145	10.5809	10.4267
Stage-3 & $\theta_2$	21.2139	17.6990	22.2106
Stage-3 & $\theta_3$	19.9361	17.5506	20.8673
Stage-3 & $\theta_4$	22.4611	19.1113	23.4249
Stage-3 & $\theta_1\theta_2$	11.8844	10.4773	10.4633
Stage-3 & $\theta_1\theta_3$	11.9228	10.5364	10.4736
Stage-3 & $\theta_1\theta_4$	11.9304	10.5626	10.4745
Stage-3 & $\theta_2\theta_3$ (c)	18.9731	16.6755	20.1005
Stage-3 & $\theta_2\theta_4$	21.1142	17.4612	21.8641
Stage-3 & $\theta_3\theta_4$	19.7323	17.4131	20.6949
Stage-3 & $\theta_1\theta_2\theta_3$	11.8025	10.4472	10.4982
Stage-3 & $\theta_1\theta_2\theta_4$	11.7619	10.4329	10.5164
Stage-3 & $\theta_1\theta_3\theta_4$	11.8245	10.4690	10.5340
Stage-3 & $\theta_2\theta_3\theta_4$	18.5591	16.5285	20.0187
Stage-3 & $\theta_1\theta_2\theta_3\theta_4$ (d)	11.6248	10.3927	10.4607

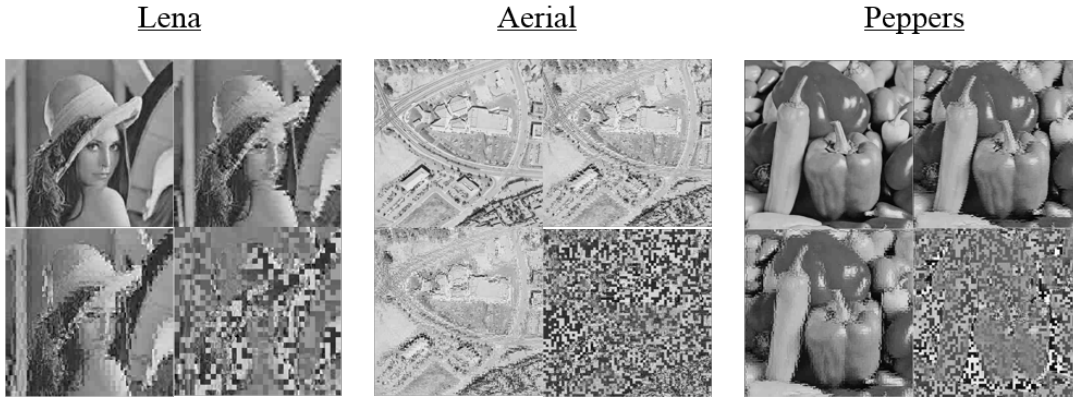


Figure 5: Encrypted images with different rotation angles change (left-top: Case (a) in Table 1; right-top: Case (b) in Table 1; left-bottom: Case (c) in Table 1; right-bottom: Case (a) in Table 1

### 224 3.3. Improved encryption scheme

225 In Fig. 3, we can observe that the encrypted image of ‘Lena’ under  
 226 *Algorithm-1* still reveals some information about the original image. Thus  
 227 in order to make encrypted image become more chaotic, we introduce the  
 228 block permutation operation after the quantization procedure, which means  
 229 that after we obtain all quantized  $8 \times 8$  blocks, before doing the entropy cod-  
 230 ing stage, we first disrupt the order of these  $8 \times 8$  blocks, according to the  
 231 encryption key. The permutation algorithm we select is Fisher-Yates Shuffle  
 232 which is used for generating a random permutation of a finite linear array  
 233 [19]. To shuffle an array  $S$  of  $n$  elements, Fisher-Yates Shuffle do

```

234   for  $i \leftarrow n$  to 2 do
235        $j \leftarrow$  random integer with  $1 \leq j \leq i$ 
236       exchange  $S[j]$  and  $S[i]$ 
237   end for

```



238 When applying this shuffle algorithm in our encryption scheme,  $S$  is the  
239 original order of all  $8 \times 8$  blocks,  $n$  is the number of  $8 \times 8$  block, the random  
240 integer in each loop is obtained from the RC4 generated pseudo-random bit-  
241 stream, which can be described as following:

242 *Random Integer Generation*

---

- 243
- 244 1. Chose an integer  $r$  satisfying  $2^r \geq n$ ;
  - 245 2. Obtain  $r$  bits from the RC4 generated key-stream and convert them to a  
246 number  $x$  such that  $0 \leq x < 2^r$ ;
  - 247 3. Compute  $t = \lfloor \frac{x}{n} \rfloor$ , and output  $x - tn$  as the random integer;
- 

248

249 We name the block permutation embedded encryption algorithm as *Algorithm-*  
250 *1'*. The corresponding encrypted Lena image is shown in Fig. 6. It is obvious  
251 that the encrypted Lena image of *Algorithm-1'* is more chaotic than that of  
252 the image encrypted by *Algorithm-1*. Moreover, because we perform the per-  
253 mutation in  $8 \times 8$  block unit, the final bit-stream size will only change slightly,  
254 which means that the good encryption and compression performances of  
255 *Algorithm-1* can be maintained.



Figure 6: Lena image encrypted by *Algorithm-1'* (left: plain image; right: cipher image)

## 256 4. Security analysis

### 257 4.1. Key space and encryption space

258 There are many possible cryptographic attacks during the decoding, such  
259 as known-plaintext attack, chosen-plaintext attack, and ciphertext-only at-  
260 tack. Among them, the ciphertext-only attack is the most realistic and basic  
261 one in which attackers can only obtain the encrypted data. Here we evaluate  
262 the effectiveness of our encryption algorithms under this type of attack.

263 One of the typical methods for ciphertext-only attack is to try all possible  
264 keys in the brute-force manner. In our algorithm, we apply the RC4 key  
265 generator with a 128-bit key, thus obtain a  $2^{128}$  key space, which is not  
266 feasible for attackers to guess. However, instead of guessing the key we use,  
267 attackers can guess the transforms we use for encryption. If we define the  
268 encryption space to denote how many rotation angles have been embedded  
269 into butterflies, then the encryption space of each  $8 \times 8$  block for *Algorithm-1*  
270 is  $2^{52}$  ( $2^4$  for all rows in the 1<sup>st</sup> dimension,  $2^6$  for each column in the 2<sup>nd</sup>  
271 dimension). Since there will be 1024 blocks with  $8 \times 8$  size in an  $256 \times 256$   
272 image, it is not feasible to try all transforms for all  $8 \times 8$  blocks. Therefore,  
273 adopting the brute-force method to recover our encrypted image is extremely  
274 difficult.

### 275 4.2. Key sensitivity analysis

276 According to Kerckhoff's principle, the security of an encryption system  
277 should rely on the secrecy of the encryption/decryption key instead of the  
278 encryption algorithm itself [20]. A good cryptosystem should be extremely

279 sensitive with respect to the key used in the algorithm, which should satisfy  
280 the following two conditions to indicate a high key sensitivity level [21]:

- 281 1) The key space should be discretized in such a way that two ciphertexts  
282 encrypted by two slightly different encryption keys should be completely  
283 different;
- 284 2) The ciphertext should not be correctly decrypted even if there is a slight  
285 difference in the encryption and decryption key.

286 If an encryption scheme satisfies the above-mentioned conditions, then its  
287 key sensitivity is considered high. In our encryption scheme, we use RC4 to  
288 generate the pseudorandom keystream which is initialized with 128-bit data,  
289 thus the 128-bit data is considered as the secret key of our cryptosystem.  
290 Overall, RC4 randomizes an array of 256 elements called  $S$ , and its output at  
291 each stage is a random element selected from  $S$ . To generate the keystream,  
292 two processes are used in RC4: a key-scheduling algorithm (KSA), which  
293 is used to initialize the permutation of  $S$ , and a pseudo-random generation  
294 algorithm (PRGA), to select the random elements and modify the original  
295 permutation of  $S$ . The pseudo-codes for the two processes are described as  
296 follows:

#### 297 **Key-scheduling algorithm**

---

```
298  
299 for  $i \leftarrow 0$  to 255 do  
300      $S[i] \leftarrow i$   
301 end for  
302  $j \leftarrow 0$   
303 for  $i \leftarrow 0$  to 255 do
```

```

304      $j \leftarrow (j + S[i] + \text{key}[i \bmod \text{keylength}]) \bmod 256$ 
305     exchange  $S[i]$  and  $S[j]$ 
306 end for

```

---

```

307
308 Pseudo-random generation algorithm

```

---

```

309
310      $i \leftarrow 0$ 
311      $j \leftarrow 0$ 
312     while GeneratingOutput do
313          $i \leftarrow (i + 1) \bmod 256$ 
314          $j \leftarrow (j + S[i]) \bmod 256$ 
315         exchange  $S[i]$  and  $S[j]$ 
316          $K \leftarrow S[(S[i] + S[j]) \bmod 256]$ 
317          $K$  as output
318     end while

```

---

319  
320 In our scheme, we use 128-bit data as the key, totally 16 decimals ranged  
321 in  $[0,255]$ , thus the *keylength* used in KSA is 16. It is obvious that any minor  
322 change in *key* will alter the initial permutation result of  $S$ , and eventually  
323 affect the output  $K$ , which determines the following new transforms selec-  
324 tion process and  $8 \times 8$  blocks' permutation result. Though we do not use the  
325 keystream to directly modify pixel values of the plainimage (like XOR op-  
326 eration between pixels and keystream bits), changes occurred in keystream  
327 will still greatly impact the final encrypted/decrypted images, which can be  
328 seen in the following two conditions' verification results.

329 To verify the first condition, we slightly modify the 16 decimals' *key* by  
 330 giving an increment of 1 to the last decimal. The correlation coefficient  
 331 between different images encrypted using original key and slightly different  
 332 key is shown in Table 2. Moreover, in Fig. 7, we have taken 'Aerial' as  
 333 an example to present the cipher images with slightly different encryption  
 334 key and the difference image of *Algorithm-1* and *Algorithm-1'*. The low  
 335 correlation coefficient and chaotic difference images prove the fulfilment of  
 336 condition 1 of key sensitivity analysis for our proposed encryption scheme.

Table 2: Correlation coefficient for image encrypted with original key and slightly different key

Image \ Algorithm	<i>Algorithm-1</i>	<i>Algorithm-1'</i>
Lena	0.0351	0.0057
Aerial	0.0201	-0.0018
Peppers	-0.0090	0.0269
Clock	0.0050	-0.0364
Resolution chart	0.0229	0.0123
Chemical plant	-0.0068	0.0014
Couple	0.0161	-0.0010
Stream and bridge	0.0094	0.0006
Sailboat	0.0011	0.0121
Baboon	-0.0009	-0.0080

337 To test the second condition, the encrypted image corresponding to plain  
 338 image is decrypted with a slightly different decryption key rather than the  
 339 original one. In our encryption scheme, we use the symmetric key system,

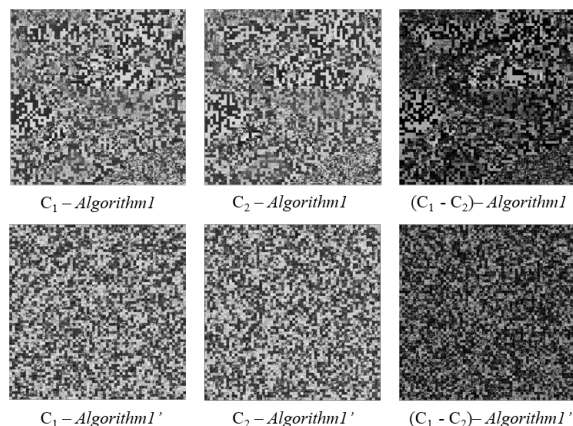


Figure 7: Key sensitivity analysis for encryption process — Encrypted 'Aerial' image with slightly modified encryption keys and their difference images

340 thus the encryption key and the decryption key are the same. We modify  
 341 the decryption key by giving an increment of 1 to the last decimal of *key*.  
 342 Decrypted images of 'Aerial' under *Algorithm-1* and *Algorithm-1'* obtained  
 343 with slightly different decryption keys are shown in Fig. 8. It is clear that  
 344 even when there is a small variation in the decryption key, the correct decryp-  
 345 tion cannot be realized under our encryption scheme. Thus, our proposed  
 346 technique also satisfies the second condition of key sensitivity analysis.

#### 347 4.3. Security against replacement attack

348 Replacement attacks are used to break multimedia encryption algorithms,  
 349 which try to recover the plain media by replacing the encrypted parameter  
 350 with the unencrypted ones or some others [22]. It can be divided into two  
 351 categories: direct replacement and correlation-based replacement. Direct  
 352 replacement means to reconstruct the plain media content by replacing some  
 353 of the encrypted data with other ones under the condition of knowing only

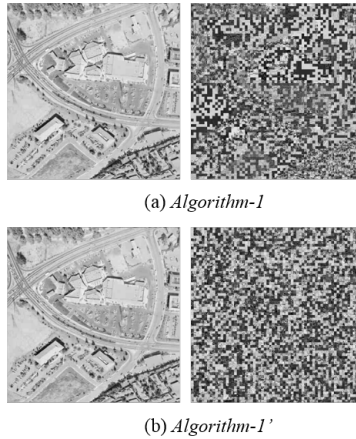
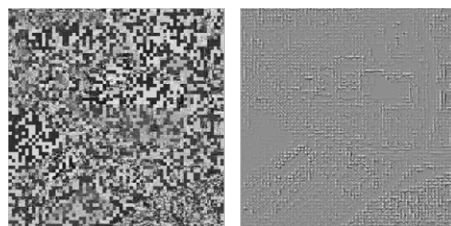


Figure 8: Key sensitivity analysis for decryption process: left image decrypted with right encryption key, right image decrypted with slightly modified decryption key

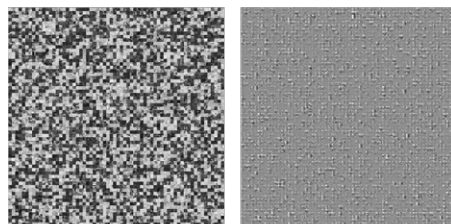
354 the cipher media content. Correlation-based replacement is similar to direct  
 355 replacement with the difference that some of the encrypted data is replaced  
 356 by unencrypted data.

357 In our proposed image encryption scheme, we realize encryption at JPEG's  
 358 transformation stage. Instead of choosing important elements to be en-  
 359 crypted, and leaving unimportant ones to be unencrypted, we do not give  
 360 them a significance level, but encrypt all of them together by changing their  
 361 signs or/and magnitudes. Thus the correlation-based replacement attack  
 362 is infeasible for attacking our scheme. We analyse our technique's security  
 363 against the direct replacement attack by assigning all dc coefficients to 128  
 364 and all ac coefficients to positive, and the corresponding data of the de-  
 365 crypted 'Aerial' images under our proposed two algorithms (*Algorithm-1*,  
 366 *Algorithm-1'*) and *Algorithm-3* in [14] are shown in Fig. 9. We can observe  
 367 that encryption with block permutation have better defense ability against

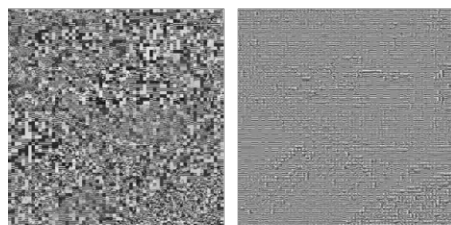
368 the direct replacement attack than encryption without block permutation  
 369 and *Algorithm-3* in [14], which both reveal some outline information about  
 370 the plain Aerial image after the direct replacement attack operation.



(a) *Algorithm-1*



(b) *Algorithm-1'*



(c) *Algorithm-3* in [14]

Figure 9: Direct replacement attack analysis for different encryption algorithms (left: encrypt image, right: decrypt image)

#### 371 4.4. Statistical model-based attack

372 Statistical model-based attack aims to recover the cipher image's intel-  
 373 ligibility under the condition of knowing only cipher images. In this kind



374 of attack, the degradation of the cipher image is reduced by using a statis-  
375 tical model [22]. The key step is to reconstruct an image with the cipher  
376 image's statistical model. If degradation of the cipher image is very strong,  
377 this attack will not work, which means that we can resist this type of attack  
378 by ensuring the low quality of our encrypted images, such as a small PSNR  
379 value.

380     Apart from the PSNR measure, attackers also can study the relationship  
381 between plain image and cipher image without knowing the encryption key  
382 to decrypt the cipher image. Generally, histograms and correlation diagrams  
383 of the original image and the encrypted image are two ways to indicate the  
384 degree of relationship between the plain image and cipher image [23–26].  
385 Histogram analysis shows the distribution of pixels in the image by counting  
386 the number of each pixel's brightness. The block permutation operation does  
387 not change pixel values, thus the histograms of encrypted image with/without  
388 permutation remain the same. In Fig. 10, we present histograms of the  
389 original 'Aerial' image and its corresponding cipher image under *Algorithm-*  
390 *1*'. It can be seen that histogram of the encrypted 'Aerial' image has little  
391 statistical similarity to that of the plain image. But the histogram does  
392 not show the normal distribution property, which indicates a more secure  
393 level, this is because our encryption scheme is based on the  $8 \times 8$  block unit,  
394 the correlation among pixels in the encrypted images cannot be destroyed  
395 completely.

396     For the correlation diagram of images, we initially identify the neighbour-  
397 hood of diagonal pixels from the original image and the encrypted image.  
398 Then 1000 pairs of two adjacent pixels are randomly selected, plot the corre-

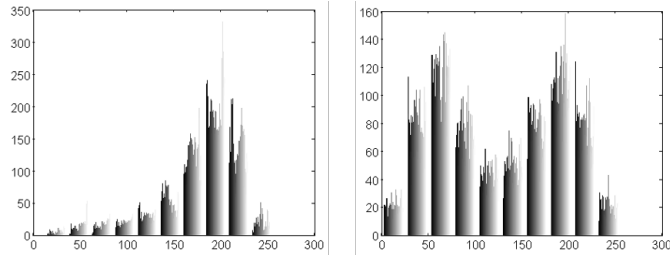


Figure 10: Histogram charts of ‘Aerial’ image (left: plain image, right: *Algorithm-1*’ encrypted image)

399 lation diagram based on the value of each pixel and its diagonal neighbours.  
 400 The corresponding diagram of ‘Aerial’ image encrypted by *Algorithm-1*’ is  
 401 shown in Fig. 11. In the original image, because the correlation between  
 402 pixels is strong, its correlation chart is shown near linear. After using the  
 403 algorithm we proposed, the linear property is not shown too much because  
 404 of the decreased correlation between pixels. However, similarly the linear  
 405 property cannot be totally removed because we realize encryption at the  
 406 transformation stage and use  $8 \times 8$  size block as permutation unit.

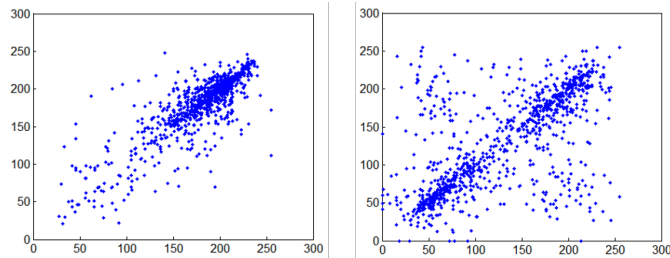


Figure 11: Diagonal correlation charts of ‘Aerial’ image (left: plain image, right: *Algorithm-1*’ encrypted image)

## 407 5. Conclusion

408 In this paper, a new joint image compression and encryption scheme is  
409 proposed to realize image encryption at JPEG's transformation stage. We  
410 want to emphasize that our proposed encryption technique does not aim  
411 at fully confidentiality, because the stage we choose to realize JPEG image  
412 encryption and the processing unit ( $8 \times 8$  size block) restrict that some inner  
413 properties of the plain image, like high information redundancy, may not be  
414 perfectly destroyed.

415 In our proposed encryption scheme, rather than only using  $8 \times 8$  DCT for  
416 block transformation, we first generate new order-8 orthogonal transforms  
417 by introducing an extra rotation angle of  $\pi$  to different stages' butterflies of  
418 DCT's flow-graph structure. Then these new transform sets are applied al-  
419 ternatively for transformation, according to the predefined secret encryption  
420 key, to realize joint image compression and encryption. Extensive experi-  
421 ments have been conducted to show that our encryption scheme can provide  
422 a sufficient level of encryption without scarifying JPEG's good compression  
423 ability too much. Moreover, by carefully selecting the number of butterflies  
424 for angle rotation, we can control the visual quality of the encrypted images.  
425 In the security analysis section, we have provided a detailed security analysis  
426 to prove the robustness of our encryption algorithms against various common  
427 attacks for multimedia encryption techniques.

428 We believe there are few extensions we can do in our following work.  
429 First, now we only consider JPEG image encryption during transformation,  
430 its security level is not so strong. Since most of the existing encryption algo-  
431 rithms are realized after this stage, like the entropy-coding stage encryption,

432 it would be therefore particularly interesting to see whether our current en-  
433 cryption scheme can be integrated into the existing ones so as to enlarge  
434 the space for encryption by one dimension. Second, currently we realize  
435 encryption by using different order-8 transforms or permuting  $8 \times 8$  blocks,  
436 the original correlation existed in these  $8 \times 8$  blocks cannot be perfectly re-  
437 moved and the diffusion property that a good cryptosystem should offer is  
438 not so strong in our current encryption scheme, therefore next we may try  
439 to perform transformation using different block size and to do permutation  
440 in small unit, perhaps the bit-plane level of image pixels, in order to improve  
441 the confusion and diffusion properties of our encryption scheme.

## 442 **References**

- 443 [1] D. R. Stinson, Cryptography: theory and practice, CRC press, 2005.
- 444 [2] A. Nag, J. P. Singh, S. Khan, S. Biswas, D. Sarkar, P. P. Sarkar, Image  
445 encryption using affine transform and xor operation, in: Signal Pro-  
446 cessing, Communication, Computing and Networking Technologies (IC-  
447 SCCN), 2011 International Conference on, IEEE, 2011, pp. 309–312.
- 448 [3] S. P. Indrakanti, P. Avadhani, Permutation based image encryption tech-  
449 nique, International Journal of Computer Applications (0975–8887) Vol-  
450 ume.
- 451 [4] M. A. Bani Younes, A. Jantan, Image encryption using block based trans-  
452 formation algorithm.
- 453 [5] A. Mitra, Y. S. Rao, S. Prasanna, et al., A new image encryption ap-

- 454       proach using combinational permutation techniques, *International Journal of Computer Science* 1 (2) (2006) 127–131.
- 455
- 456 [6] A. Massoudi, F. Lefebvre, C. De Vleeschouwer, B. Macq, J.-J. Quisquater, Overview on selective encryption of image and video: challenges and perspectives, *EURASIP Journal on Information Security* 2008 (2008) 5.
- 457
- 458
- 459
- 460 [7] L. Tang, Methods for encrypting and decrypting mpeg video data efficiently, in: *Proceedings of the fourth ACM international conference on Multimedia*, ACM, 1997, pp. 219–229.
- 461
- 462
- 463 [8] L. Qiao, K. Nahrstedt, M.-C. Tam, Is mpeg encryption by using random list instead of zigzag order secure?, in: *Consumer Electronics, 1997. ISCE'97., Proceedings of 1997 IEEE International Symposium on*, IEEE, 1997, pp. 226–229.
- 464
- 465
- 466
- 467 [9] C.-P. Wu, C. J. Kuo, Design of integrated multimedia compression and encryption systems, *Multimedia, IEEE Transactions on* 7 (5) (2005) 828–839.
- 468
- 469
- 470 [10] C.-P. Wu, C.-C. J. Kuo, Fast encryption methods for audiovisual data confidentiality, in: *Information Technologies 2000, International Society for Optics and Photonics*, 2001, pp. 284–295.
- 471
- 472
- 473 [11] C.-P. Wu, C.-C. J. Kuo, Efficient multimedia encryption via entropy codec design, in: *Photonics West 2001-Electronic Imaging, International Society for Optics and Photonics*, 2001, pp. 128–138.
- 474
- 475

- 476 [12] M. Van Droogenbroeck, R. Benedett, Techniques for a selective encryp-  
477 tion of uncompressed and compressed images, in: *Advanced Concepts*  
478 *for Intelligent Vision Systems (ACIVS)*, 2002.
- 479 [13] B. Zeng, S.-K. A. Yeung, S. Zhu, M. Gabbouj, Perceptual encryption of  
480 h. 264 videos: Embedding sign-flips into the integer-based transforms,  
481 *Information Forensics and Security, IEEE Transactions on* 9 (2) (2014)  
482 309–320.
- 483 [14] S.-K. A. Yeung, S. Zhu, B. Zeng, Perceptual video encryption using  
484 multiple  $8 \times 8$  transforms in h. 264 and mpeg-4, in: *Acoustics, Speech*  
485 *and Signal Processing (ICASSP)*, 2011 IEEE International Conference  
486 on, IEEE, 2011, pp. 2436–2439.
- 487 [15] S.-K. A. Yeung, S. Zhu, B. Zeng, Design of new unitary transforms for  
488 perceptual video encryption, *Circuits and Systems for Video Technology,*  
489 *IEEE Transactions on* 21 (9) (2011) 1341–1345.
- 490 [16] S.-K. A. Yeung, S. Zhu, B. Zeng, Partial video encryption based on  
491 alternating transforms, *Signal Processing Letters, IEEE* 16 (10) (2009)  
492 893–896.
- 493 [17] W.-H. Chen, C. Harrison, S. Fralick, A fast computational algorithm for  
494 the discrete cosine transform, *communications, IEEE Transactions on*  
495 25 (1977) 1004–1011.
- 496 [18] K. Kaukonen, R. Thayer, A stream cipher encryption algorithm arcfour  
497 (1999).

- 498 [19] R. A. Fisher, F. Yates, Statistical tables for biological, agricultural and  
499 medical research, Longman, 1938.
- 500 [20] A. A. Bruen, M. A. Forcinito, A. G. Konheim, C. Cobb, A. Young,  
501 M. Yung, D. Hook, Applied cryptography: protocols, algorithms, and  
502 source code in c.
- 503 [21] N. Taneja, B. Raman, I. Gupta, Combinational domain encryption for  
504 still visual data, Multimedia tools and applications 59 (3) (2012) 775–  
505 793.
- 506 [22] S. Lian, Multimedia content encryption: techniques and applications,  
507 CRC press, 2008.
- 508 [23] S. Bahrami, M. Naderi, Encryption of multimedia content in partial en-  
509 cryption scheme of dct transform coefficients using a lightweight stream  
510 algorithm, Optik-International Journal for Light and Electron Optics  
511 124 (18) (2013) 3693–3700.
- 512 [24] S. S. Agaian, R. G. Rudraraju, R. C. Cherukuri, Logical transform based  
513 encryption for multimedia systems, in: Systems Man and Cybernetics  
514 (SMC), 2010 IEEE International Conference on, IEEE, 2010, pp. 1953–  
515 1957.
- 516 [25] W. Li, N. Yu, A robust chaos-based image encryption scheme, in: Mul-  
517 timedia and Expo, 2009. ICME 2009. IEEE International Conference  
518 on, IEEE, 2009, pp. 1034–1037.
- 519 [26] G. Chen, Y. Mao, C. K. Chui, A symmetric image encryption scheme

520 based on 3d chaotic cat maps, *Chaos, Solitons & Fractals* 21 (3) (2004)  
521 749–761.